ZEOLITE CRYSTAL GROWTH

(ZCG)

FLIGHT ON USML-2

FINAL REPORT

NASA CONTRACT NO : NAS8-40260

BY

ALBERT SACCO JR [1]
NURCAN BAC [1]
JULIUSZ WARZYWODA [1]
IPEK GURAY [2]
MICHELLE MARCEAU [2]
TERAN L. SACCO [2]
LEAH M. WHALEN [2]

1. Chemical Engineering Department, Northeastern University
342 Snell Engineering Center
Boston, MA 02115

2. Chemical Engineering Department, Worcester Polytechnic Institute
100 Institute Rd.
Worcester, MA 01609

AUGUST 1997

TABLE OF CONTENTS

1.0 ABSTRACT

The extensive use of zeolites and their impact on the world's economy has resulted in many efforts to characterize their structure, and improve the knowledge base for nucleation and growth of these crystals. The zeolite crystal growth (ZCG) experiment on USML-2 aimed to enhance the understanding of nucleation and growth of zeolite crystals, while attempting to provide a means of controlling the defect concentration in microgravity. Zeolites A, X, Beta, and Silicalite were grown during the 16 day - USML-2 mission. The solutions where the nucleation event was controlled yielded larger and more uniform crystals of better morphology and purity than their terrestrial/control counterparts. The external surfaces of zeolite A, X, and Silicalite crystals grown in microgravity were smoother (lower surface roughness) than their terrestrial controls. Catalytic studies with zeolite Beta indicate that crystals grown in space exhibit a lower number of Lewis acid sites located in micropores. This suggests fewer structural defects for crystals grown in microgravity. Transmission electron micrographs (TEM) of zeolite Beta crystals also show that crystals grown in microgravity were free of line defects while terrestrial/controls had substantial defects.

2.0 INTRODUCTION

Zeolites are crystalline aluminosilicates. These materials have an open framework based on an extensive three dimensional network of oxygen ions. Situated within the tetrahedral sites formed by the oxygen can be either an Al^{+3} or Si^{+4} ion. This unique structure has proved to be extremely effective in processing materials at the molecular level and led to zeolites becoming the backbone of chemical and petrochemical process industries. The extensive use of zeolites in refining (gasoline production by Fluidized Catalytic Cracking (FCC)), petrochemical processing, laundry detergents, agriculture, and environmental cleanup as catalysts, adsorbents and ion exchangers caused the market to mushroom in mid-1980's, reaching a worldwide sales of about 2 billion dollars. The existing markets for zeolites are expected to grow at a rate of 3-4% through 2000 (1). Continued growth for zeolites includes cultivating markets beyond petroleum refining, and detergents. New applications for these molecularly selective materials are in areas such as selective membranes, chemical sensors, molecular electronics, quantum-confined semiconductors and zeolite-polymer composites.

The importance of zeolites has driven extensive efforts to characterize their structures and understand their nucleation and growth mechanisms. These efforts aim to be able to produce "custom-made" zeolites tailored for a desired application. To date, nucleation mechanisms and growth are not well understood for many of the systems involved. In most cases, the problem is compounded with the presence of a gel phase that controls the degree of supersaturation. This gel also undergoes a continuous polymerization type reaction during nucleation and growth. Currently, there is no available technology to grow large, crystallographically perfect zeolites in high yield. The microgravity environment on board the space shuttle in low earth orbit provides a

unique environment (around 10^{-4} - 10^{-6} g) for zeolite crystal growth. This environment virtually eliminates settling and convection, enhances diffusion-limited growth, and reduces collision breeding. These benefits led to several attempts to grow larger and structurally improved zeolites in space (2-5) providing mixed results in literature. The previous attempts of Sacco *et. al* (6) indicated that larger zeolite crystals with fewer defects can be synthesized in microgravity. Investigating zeolite crystal growth in microgravity enhances the understanding in nucleation and growth mechanisms. This also provides a means to control the defect structure in crystals grown in space. Availability of larger crystals with a controlled defect structure is expected to improve the existing applications as well as providing new areas of use.

3.0 RESULTS

Four different zeolite types were crystallized during the USML-2 mission. The results for zeolites A, X, Beta and Silicalite are reported here. The zeolite crystals grown in micrograviy and their terrestrial/controls are compared with techniques including Scanning Electron Microscopy (SEM), Particle Size Distribution (PSD), X-Ray Diffraction (XRD), Transmission Electron Microscopy (TEM), Microprobe analysis, and Fourier Transform Infrared (FTIR). The results of catalytic activities in reactions using the Silicalite and the zeolite Beta crystals are reported.

3.1 Zeolite A

Figures 1 and 2 show typical results from zeolite A synthesis using the nucleation control agent triethanolamine (TEA). The SEM micrographs in Figure 1 indicate that the largest flight Zeolite A crystals (85 μm cubes) are 70% larger in linear dimension than the largest terrestrial zeolite A crystals with sizes up to 50 μm. This linear size increase corresponds to about 190 % increase in the surface area, and 390 % increase in the volume of zeolite A crystal. Particle size distributions (PSD's) of these flight and terrestrial products shown in Figure 2 are in agreement with the SEM micrographs. These show that a considerable population of large zeolite A crystals exists in the flight sample. The shape of PSD is different for flight and terrestrial sample indicating different nucleation and/or growth history for these samples. It should be noted that the sizes of zeolite A crystals grown during USML-2 and their terrestrial counterparts show a substantial improvement over commercial zeolite A products, and previous USML-1 flight results. Our increased zeolite crystallization knowledge through space flight led us to be able to produce terrestrial zeolite A crystals during USML-2 that are equal or larger in size than those produced during USML-1 flight.

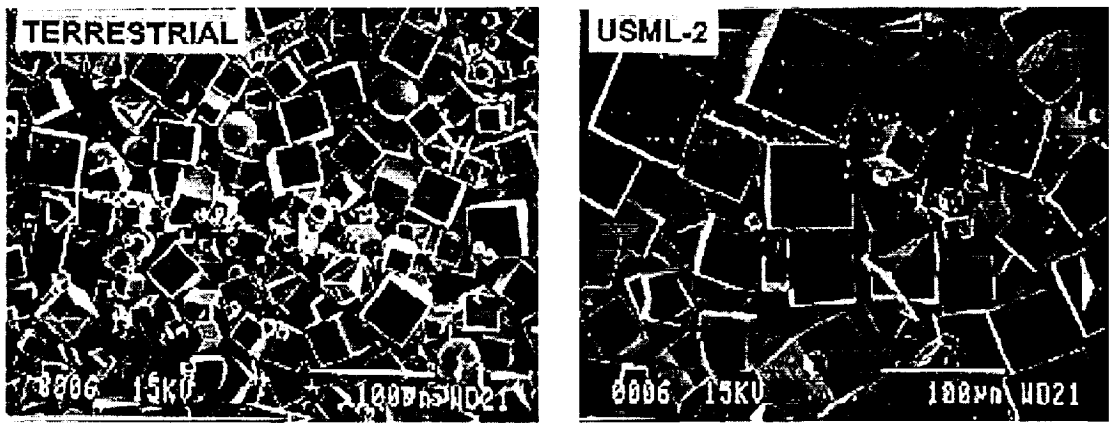

Figure 1. SEM Micrographs of Zeolite A Using TEA as a Nucleation Control Agent

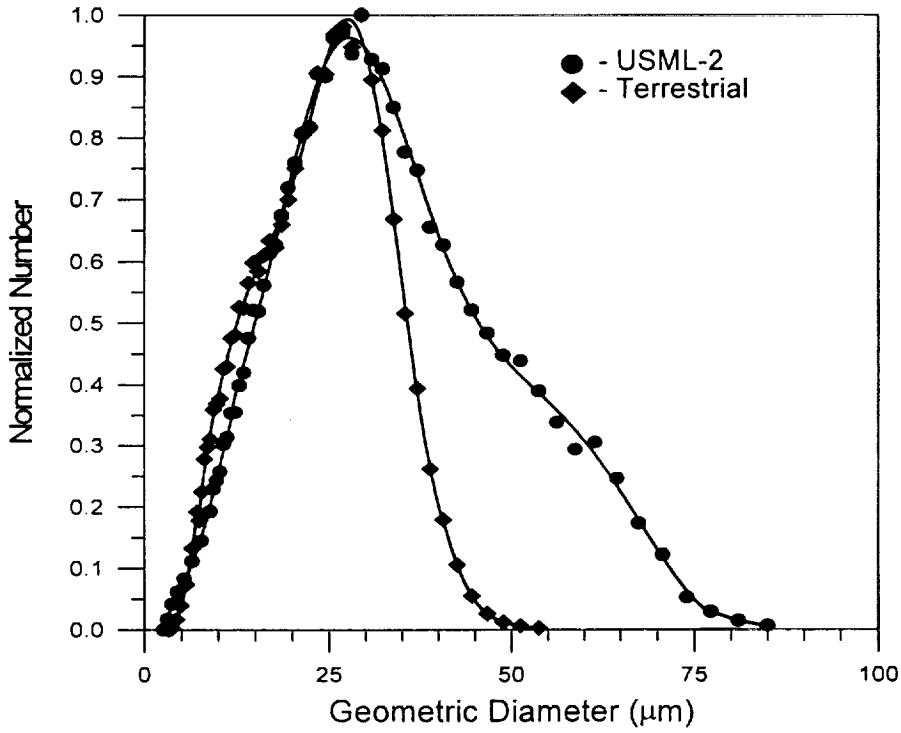

Figure 2. PSD's of Zeolite A Illustrated in Figure 1

Figure 3 shows the improvements in zeolite A crystallization with SEM micrographs of commercial, USML-1, and USML-2 crystals at the same magnification. The large zeolite A crystals (~85 μm) in the USML-2 product are about 42 times greater than the commercial crystals (~2 μm). This corresponds to a volume increase of about 77,000 times for the flight crystals over the commercial crystals. Figure 4 illustrates the PSD's for the samples shown in Figure 3.

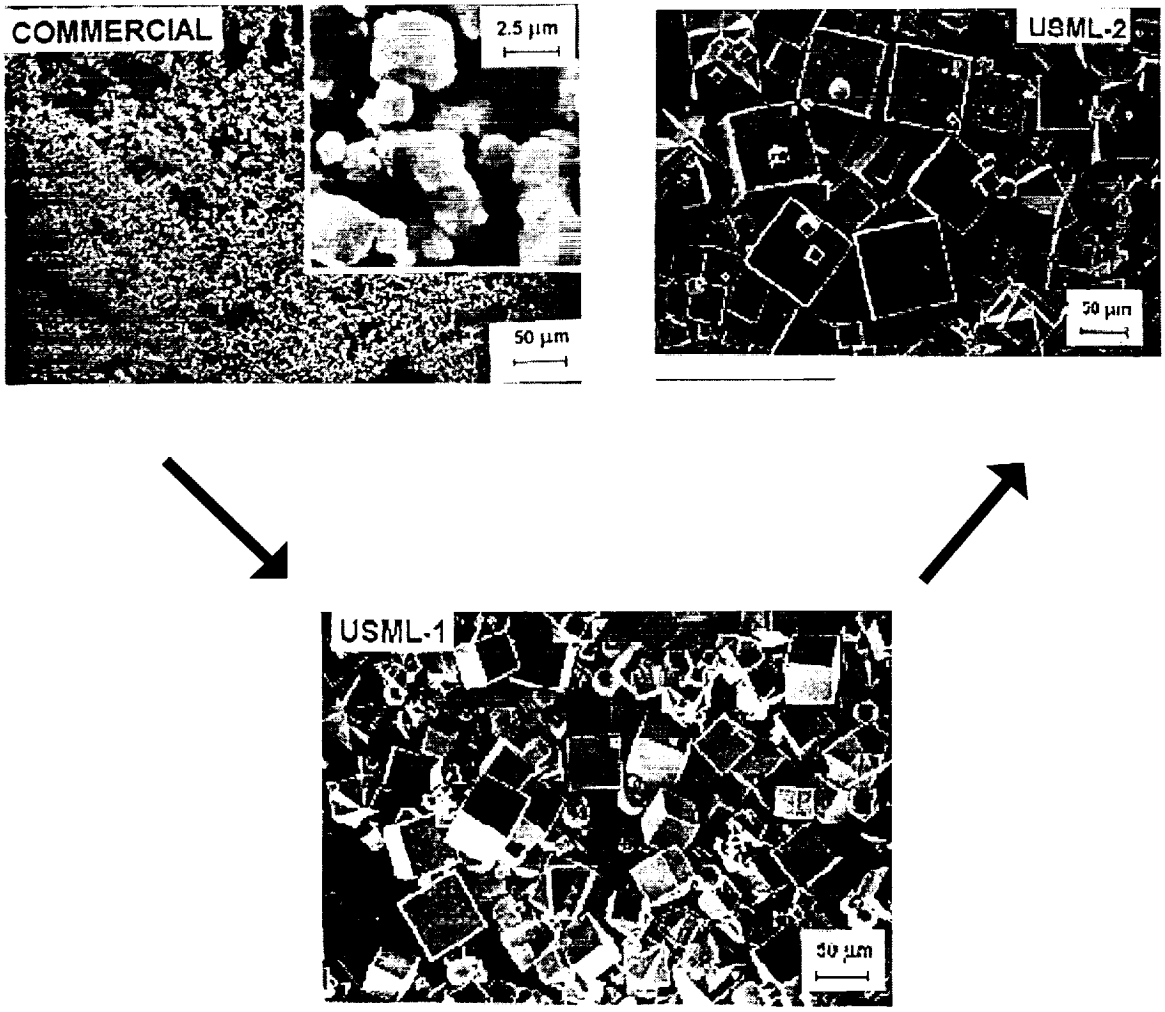

Figure 3. Improvements from Space Research - Zeolite A

Figures 5 and 6 show typical results from zeolite A synthesis using the nucleation control agent 2,2-Bis(hydroxymethyl)-2,2',2"-nitrilotriethanol (BIS). Figure 6 shows that the flight crystals are 40-60 % larger than the terrestrial/control crystals, and indicate that the presence of an amorphous phase in addition to zeolite A crystals in the flight sample. The amorphous phase corresponds to unreacted species (gel) which given enough time at reaction temperature will allow the flight sample to grow even larger. The corresponding terrestrial sample is free from unreacted amorphous material. These differences indicate possibility of slower crystallization rates of zeolite A in microgravity. PSD's for these samples shown in Figure 6 confirm the size differences between the flight and terrestrial/control samples seen in Figure 5 and clearly indicate the presence of an amorphous material in the flight sample manifested as a second peak centered around 5 μm.

Table 1 shows the comparison of lattice parameters for flight and terrestrial (control) samples in a typical zeolite A experiment. As illustrated, the lattice parameters and, thus, the unit cell volumes for the flight samples were frequently smaller than for the terrestrial counterparts. This is consistent with fewer lattice defects in the structure, and is consistent with similar results for Spacehab-1 and USML-1.

Table 1. XRD Data Comparing Flight (F) and Terrestrial/Control (T) Zeolite A samples

Sample	a (Å)	Volume ($Å^3$)
F (TEA)	12.27±0.01	1848.97
T (TEA)	12.29±0.00	1857.10
F (BIS)	12.30±0.00	1863.23
T (BIS)	12.31±0.00	1866.82

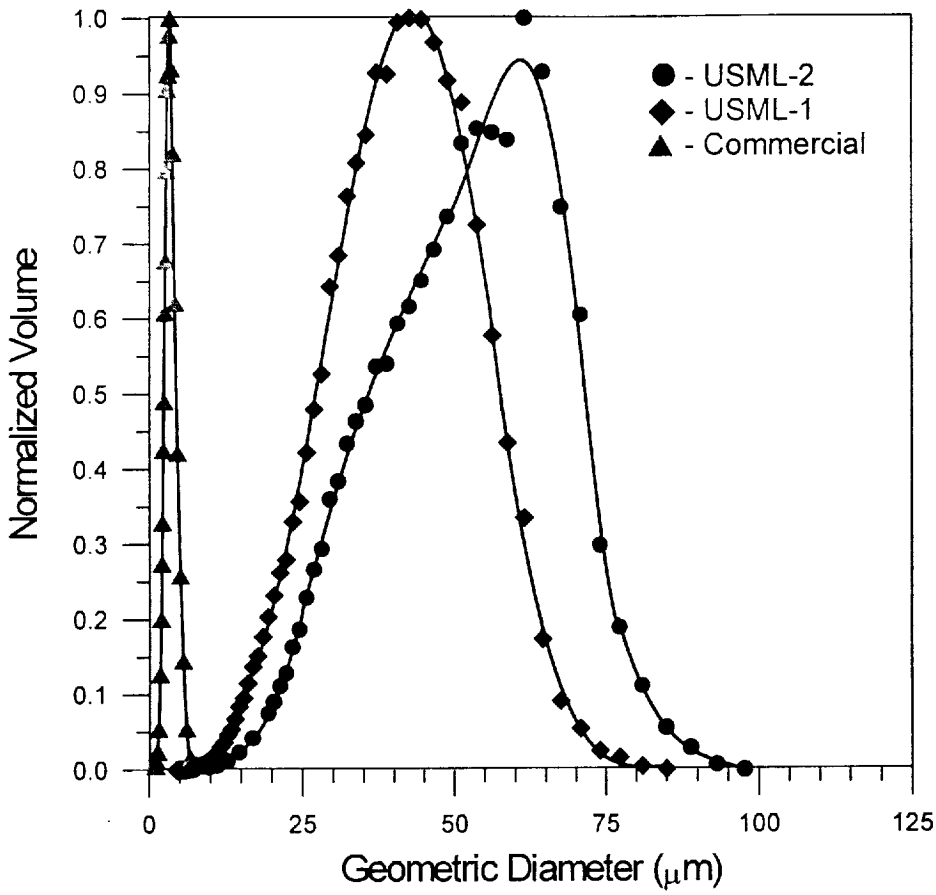

Figure 4. PSD's of Commercial, USML-1, and USML-2 Zeolite A Crystals

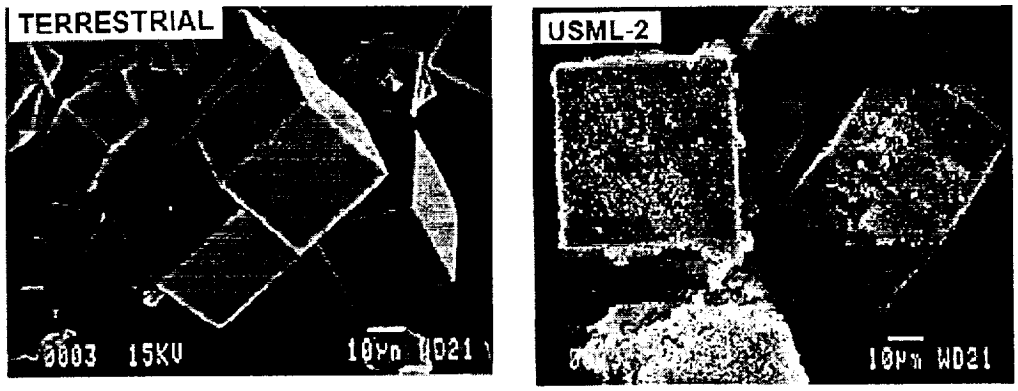

Figure 5. SEM Micrographs of Zeolite A with BIS Indicating Unreacted Gel

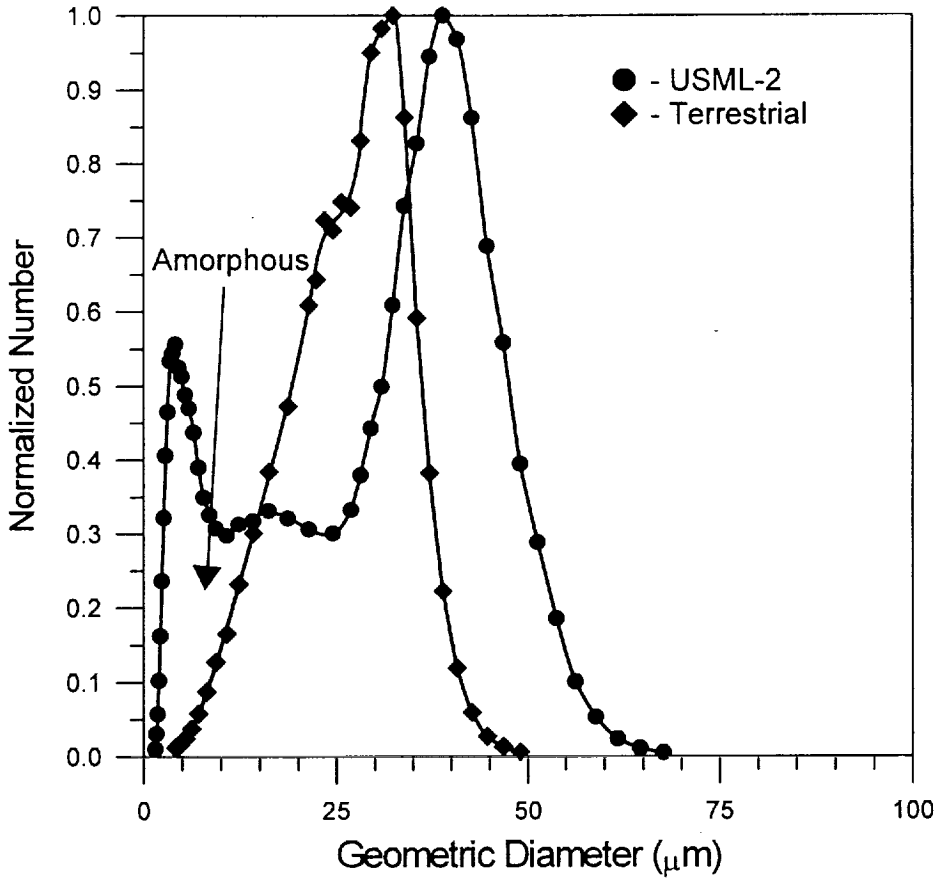

Figure 6. PSD's of Zeolite A Illustrated in Figure 5

Figure 7 shows the Atomic Force Microscope (AFM) micrographs of Zeolite A crystals using BIS as the nucleation control agent at two different magnifications. These micrographs clearly indicate a much smoother surface for crystals grown in space. The space grown crystal on the right hand side of Figure 7 indicates regular layerwise growth for Zeolite A crystal. The terrestrial/control counterpart on the left hand side, however, exhibits a rough surface with an unusual "liquid-like" surface structure.

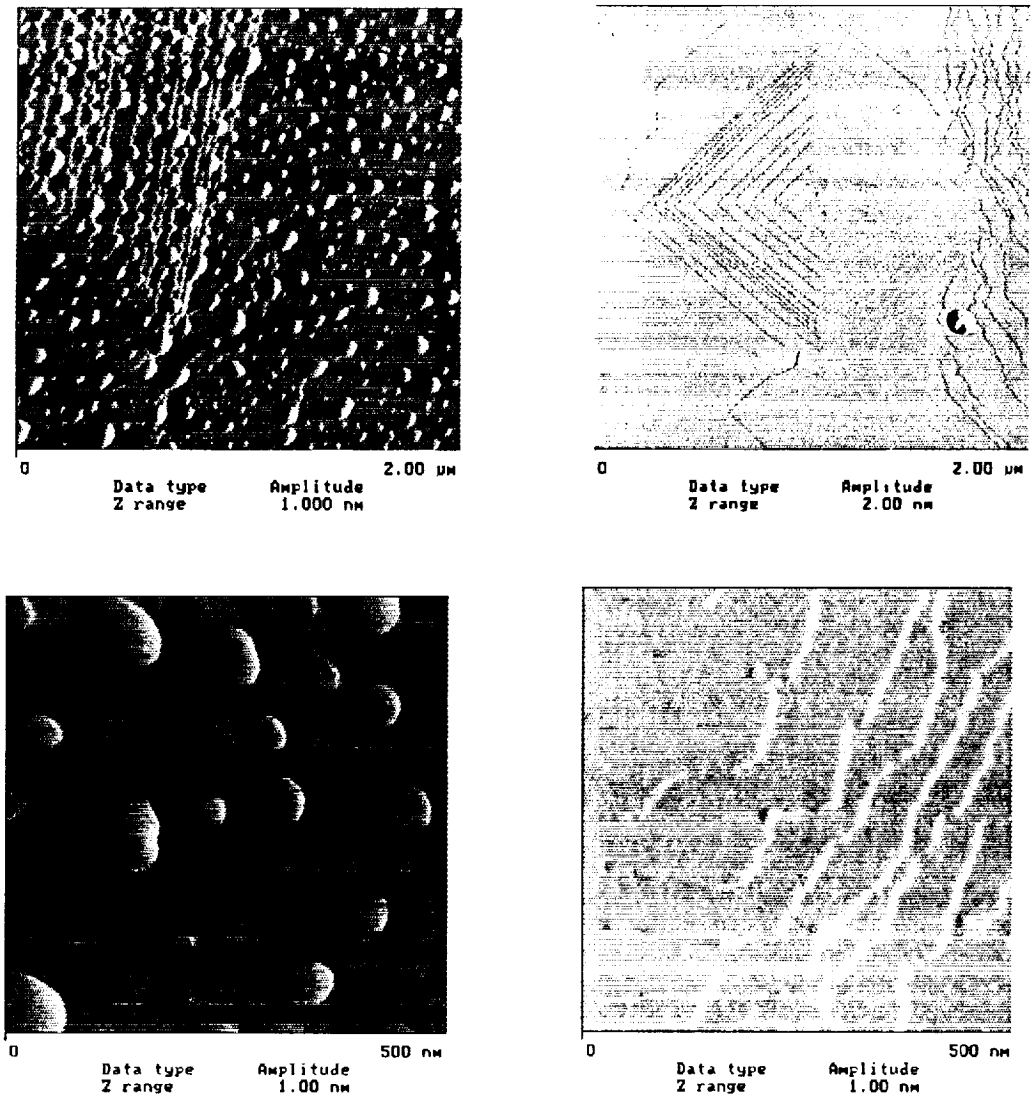

Figure 7. AFM Micrographs of Zeolite A Using BIS as a Nucleation Control Agent

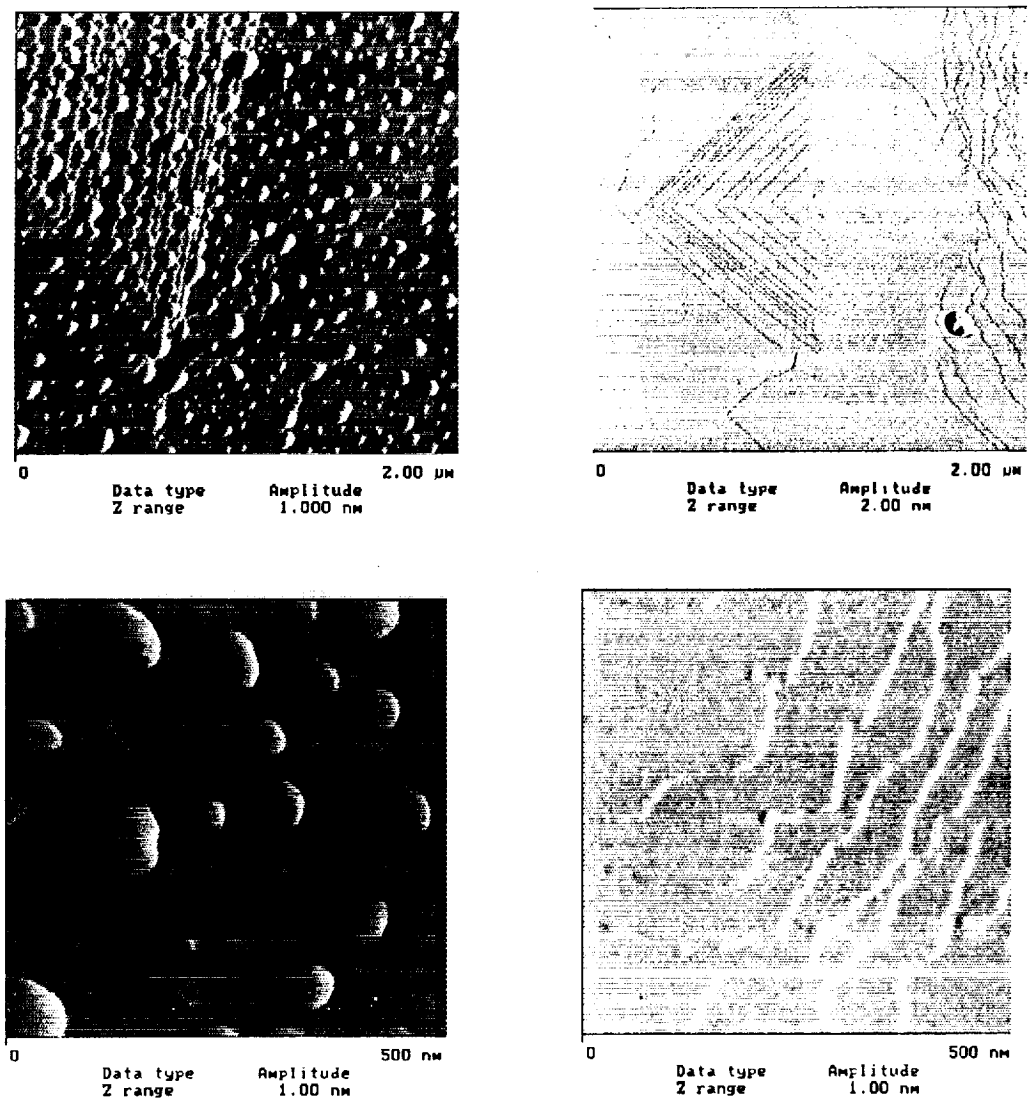

Figure 7. AFM Micrographs of Zeolite A Using BIS as a Nucleation Control Agent

3.2 Zeolite X

Figures 8 and 9 show typical results from zeolite X formulations using the nucleation control agent TEA. SEM micrographs (Figure 8) indicate that largest flight zeolite X crystals (octahedra with side ~215 μm) are about 35% larger in linear dimension than largest terrestrial/control zeolite X crystals with side ~160 μm. This linear size increase corresponds to about 81 % increase in the surface area, and about 143 % increase in the volume of zeolite X crystal. The increases in surface area and volume are significant for certain applications, such as incorporating semiconductors into cages in the zeolite framework (e.g., quantum dots).

The PSD's of these flight and terrestrial/control samples, shown in Figure 9, are in agreement with the SEM micrographs and confirm a significant shift to larger sizes for crystals grown in microgravity. Other formulations using less TEA resulted in a similar 30-40% increase of linear dimension of flight zeolite X crystals in comparison to their terrestrial/control counterparts..

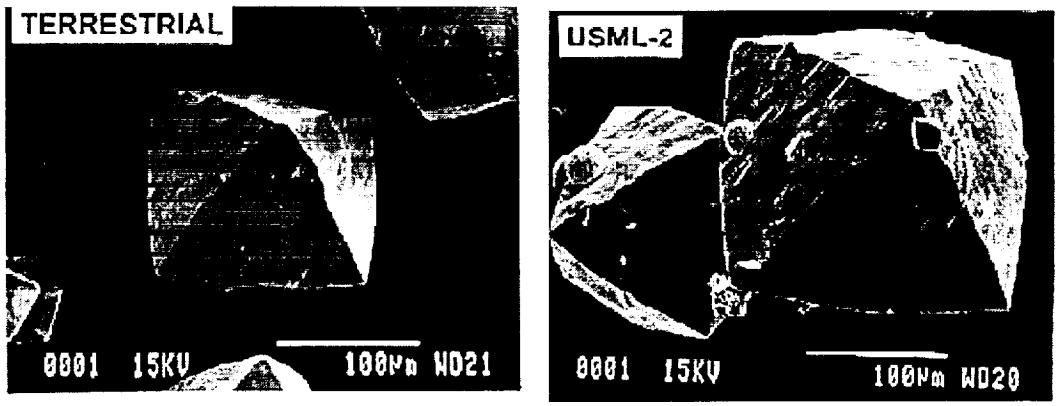

Figure 8. SEM Micrographs of Zeolite X Using TEA as a Nucleation Control Agent

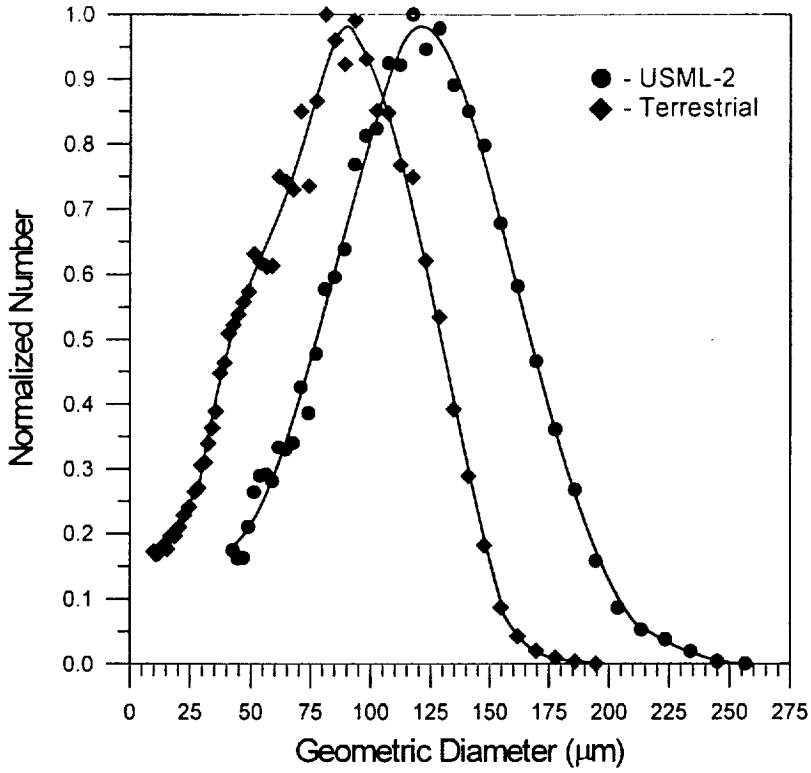

Figure 9. PSD's of Zeolite X Illustrated in Figure 8

The SEM micrographs and PSD's for other formulations are shown in Figures 10 and 11, respectively. Both scanning electron microscopy and particle size analysis show that substantially larger product is obtained in microgravity. SEM micrographs indicate that flight crystals are predominantly pure, while the terrestrial/control samples have considerable amounts of zeolite A and clusters of zeolite R and P impurity phases.

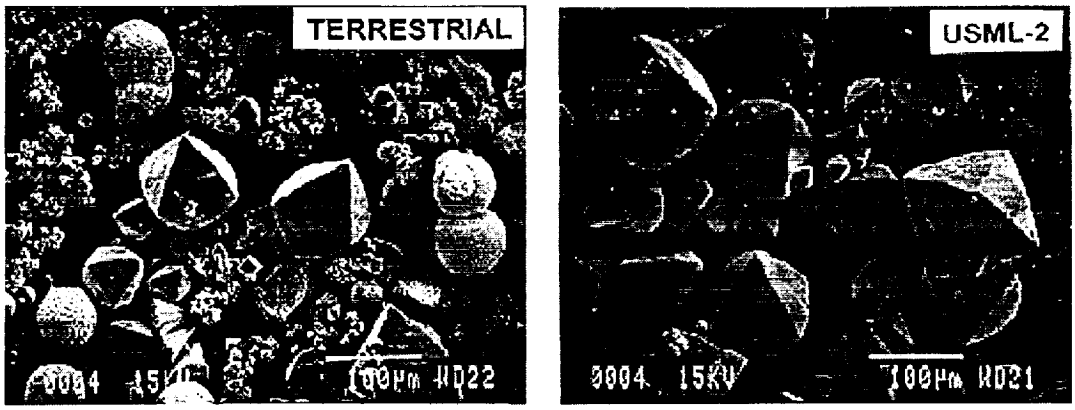

Figure 10. SEM Micrographs of Zeolite X Using TEA - Different Formulation

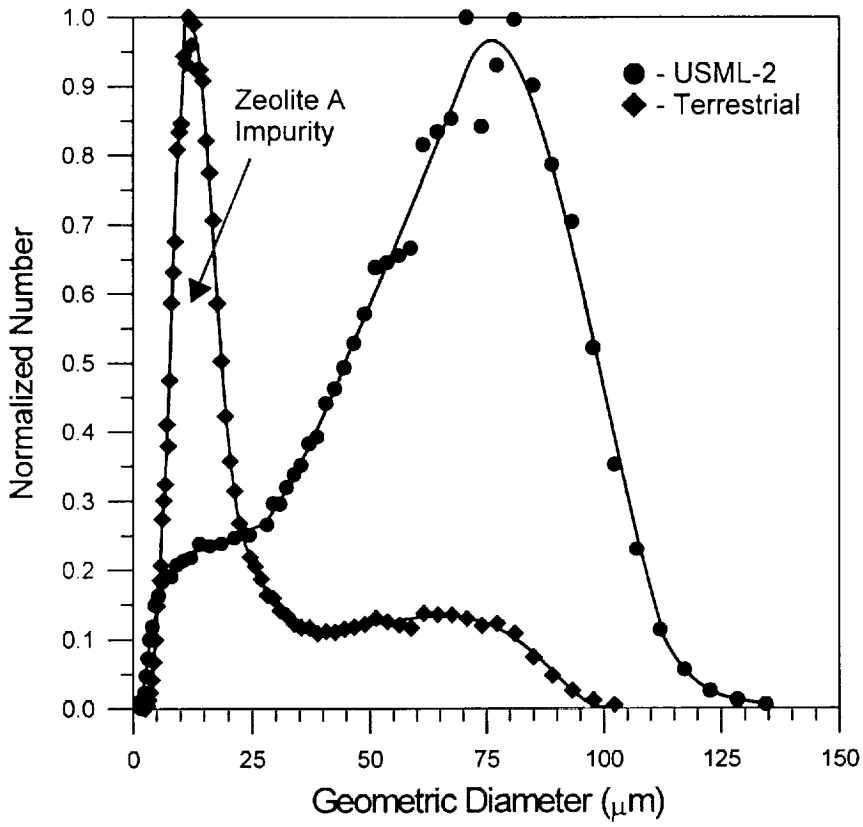

Figure 11. PSD's of Zeolite X Illustrated in Figure 10

The presence of impurities is also indicated in the PSD's in Figure 11 showing bimodal distributions for the control samples. X-ray powder diffraction (XRD) analysis confirmed the presence of impurities indicated by SEM and PSD's. The XRD patterns for crystals grown in space exhibit very sharp peaks indicating a very pure product consisting

of large single crystals. The terrestrial samples have considerable peak broadening of additional peaks due to polycrystalline impurities.

Figure 12 illustrates the improvements in zeolite X crystallization with SEM micrographs of commercial, USML-1, and USML-2 crystals at the same magnification. The particle size of zeolite X produced during the USML-2 mission is about 107 times larger than the commercial product. This corresponds to a volume increase of about 1.24 million times for the flight crystals over the commercial product.

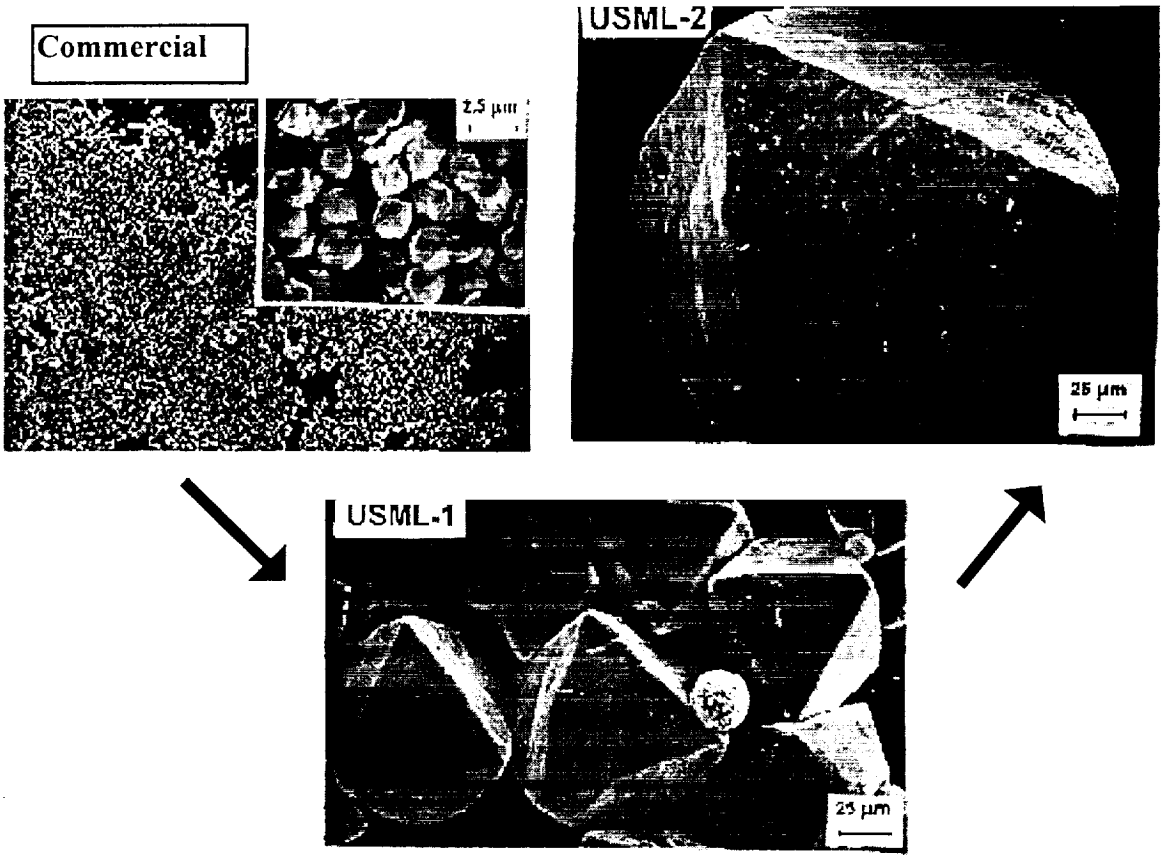

Figure 12. Improvements from Space Research - Zeolite X

Figure 13 shows PSD's of the products depicted in Figure 12. Figure 13 indicates a substantial increase of the size of crystals produced during the USML-2 mission in comparison to USML-1 and commercial zeolite X (7).

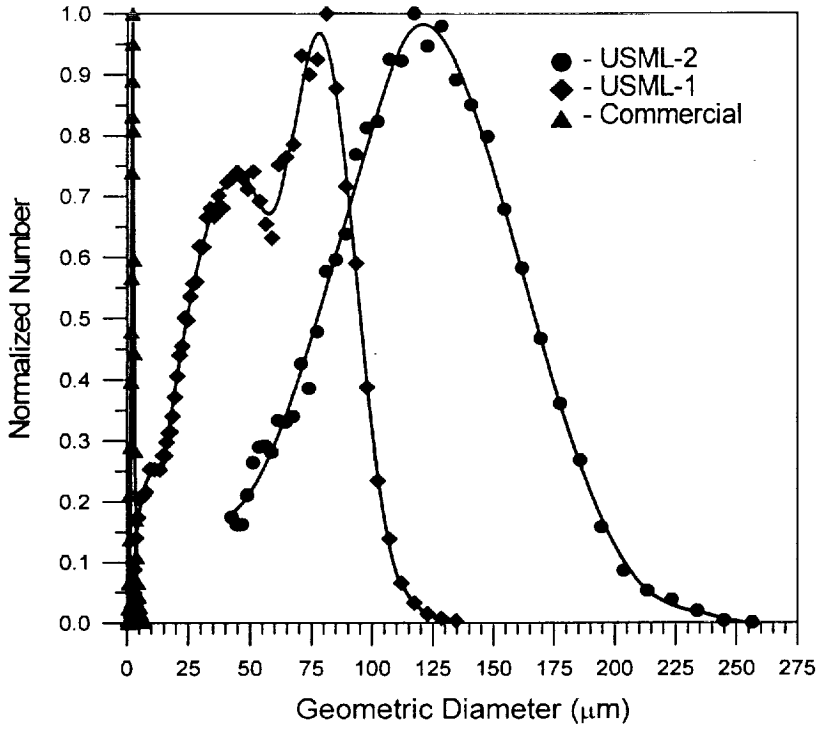

Figure 13. PSD's of Commercial, USML-1, and USML-2 Zeolite X Crystals

Figures 14 and 15 show results from another zeolite X formulation using the nucleation control agent TEA. The SEM micrographs in Figure 14 and PSD's in Figure 15 indicate that the flight zeolite X product contains zeolite A impurity, however, the flight zeolite X crystal size increase over terrestrial/control counterpart is about 70% (120 μm flight vs. 70 μm control). These results are very similar to USML-1 results obtained with similar formulation (8).

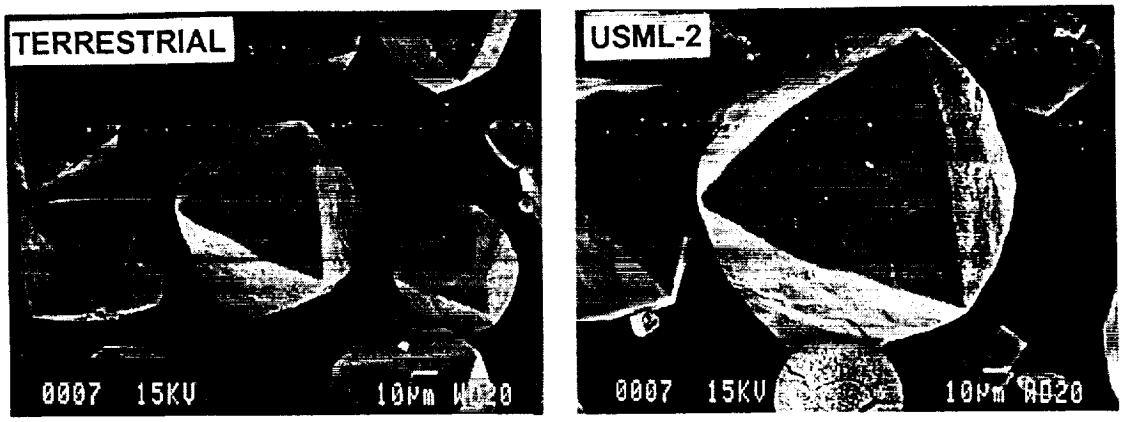

Figure 14. SEM Micrographs of Zeolite X Using TEA - Different Formulation

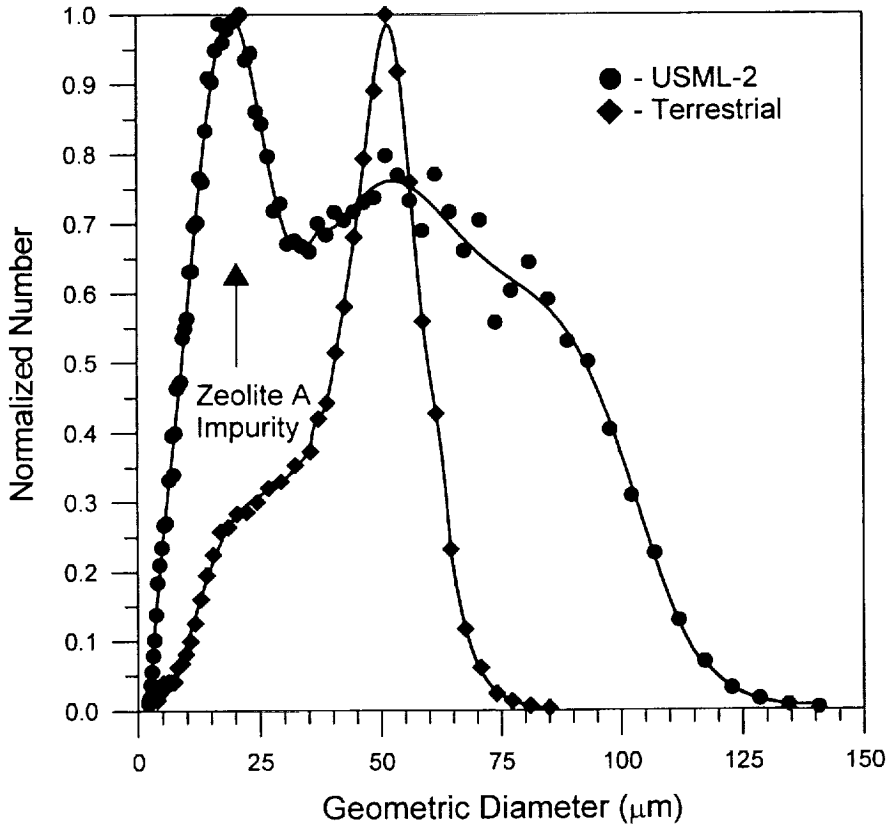

Figure 15. PSD's of Zeolite X Illustrated in Figure 14

Figure 16 shows the results of a microprobe analysis of the hexagonal cross-sections of a flight sample and its control (Figure 17). The results indicate the distribution of Al in both samples. The increase of Si/Al ratio from the center to the

exterior of crystals suggests depletion of Al in reaction mixture in agreement with the fact that Al is a limiting reagent in zeolite X synthesis (9). As shown in Figure 16 the Si/Al ratio is higher for flight sample than for the terrestrial counterpart, consistent with USML-1 results showing average Si/Al ratios larger in flight samples than in their terrestrial/control counterparts. Also, the Si/Al ratio of the flight material appears to be more uniform throughout the center of the crystal. Table 2 shows the comparison of lattice parameters for flight and terrestrial sample shown in Figure 17. As illustrated, the lattice parameters and, thus, the unit cell volumes for the flight sample are smaller than for the terrestrial counterpart, what is consistent with its lower Al content.

Table 2. XRD Data Comparing Flight (F) and Terrestrial/Control (T) Zeolite X samples

Sample	a (Å)	ESD	Volume (Å^3)
F	24.849	0.002	15343.25
T	24.855	0.0009	15354.41

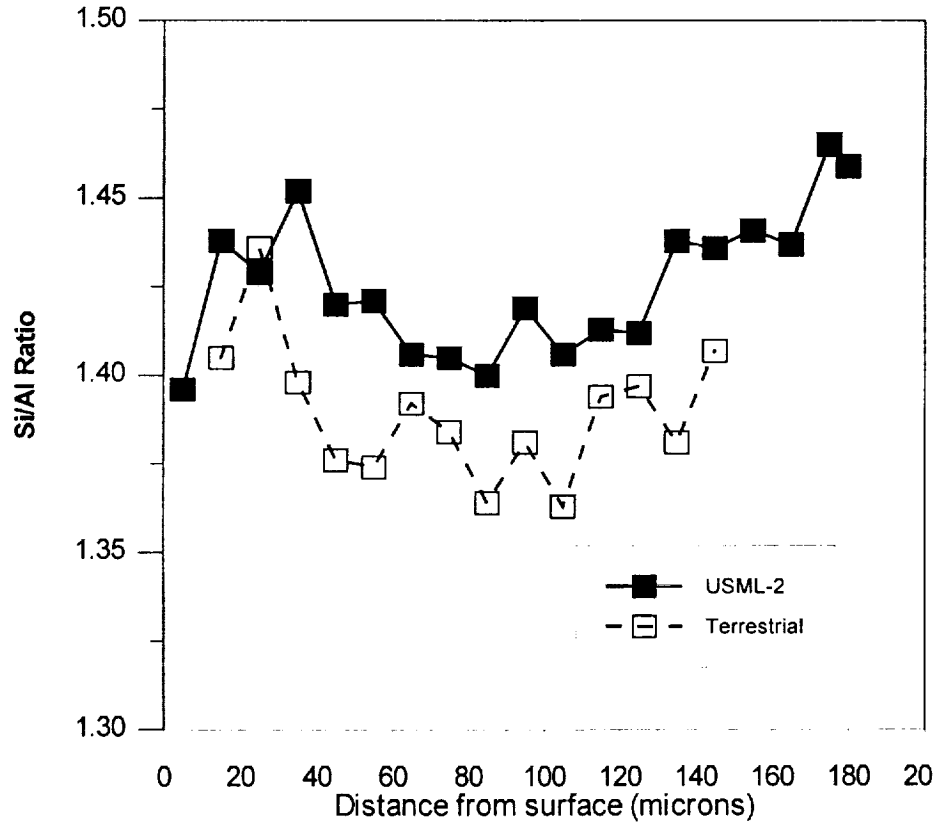

Figure 16. Si/Al Ratio by Microprobe Analysis of Zeolite X

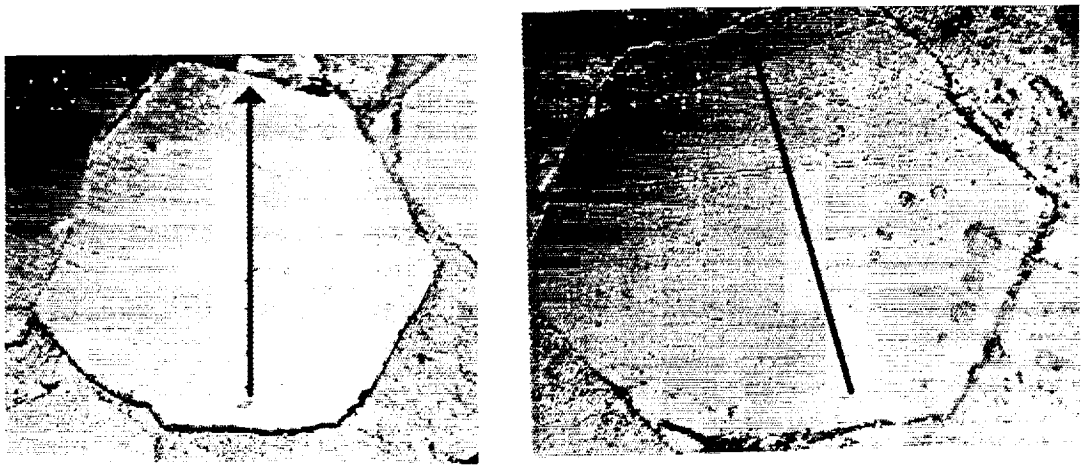

Figure 17. Cross Sections used in Microprobe Analysis

Figure 18 shows the AFM micrographs of Zeolite X using TEA as the nucleation control agent. Figure 18 indicates that the space grown Zeolite X crystal shown on the right hand side have a much "smoother" surface that the terrestrial crystal.

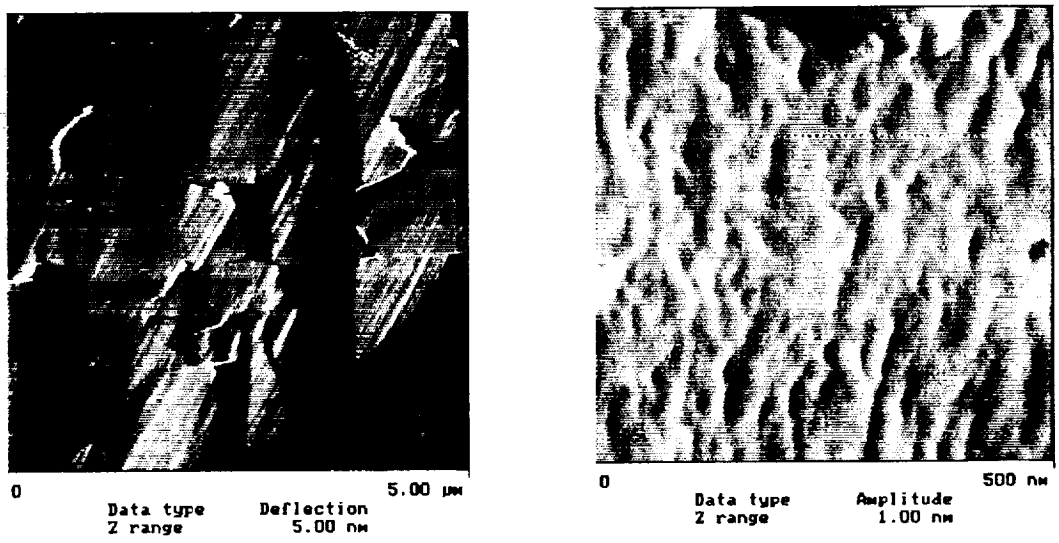

Terrestrial **USML-2**

Figure 18 AFM Micrographs of Zeolite X Using TEA as a Nucleation Control Agent

3.3 Silicalite

Figures 19 and 20 illustrate typical results from the Silicalite synthesis using untreated silica gel (without nucleation control). SEM micrographs shown in Figure 18 indicate clearly that the intergrown disks morphology of Silicalite crystals grown in microgravity is different from the morphology of Silicalite crystals grown in a 1g environment. The terrestrial crystals were in the form of spherulitic agglomerates.

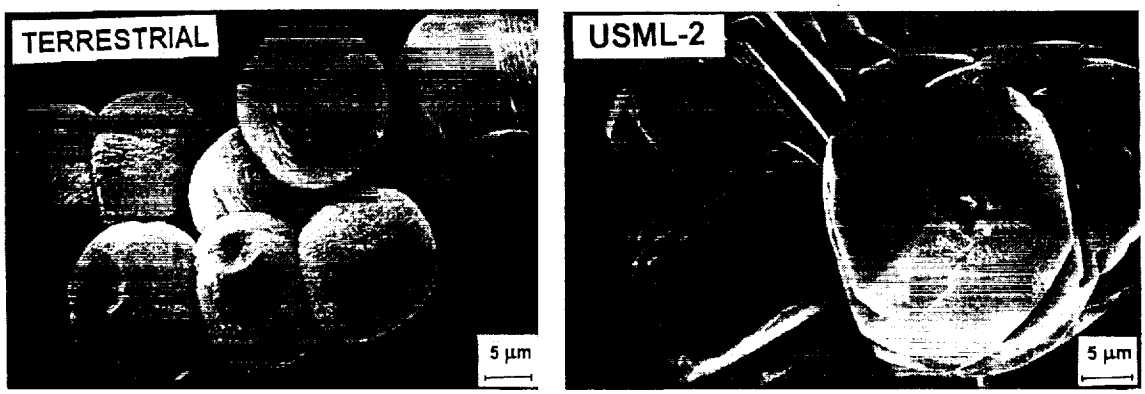

Figure 19. SEM Micrographs of Silicalite from Untreated Silica Gel

Although the morphologies are very different for crystals synthesized in µg and 1g environments, XRD patterns for these products, indicate that they both are pure Silicalite. The PSD's for the products corresponding to Figure 19 are given in Figure 20. Figure 20 shows that the PSD of the Silicalite crystals grown in microgravity is distinctly shifted to larger geometrical diameters in comparison to PSD of Silicalite crystals grown in 1g environment. These results illustrate that when one compares the nucleation and crystal growth processes for Silicalite grown in microgravity and 1g environment, the microgravity limits or slows nucleation resulting in fewer but larger crystals with different (better) morphology.

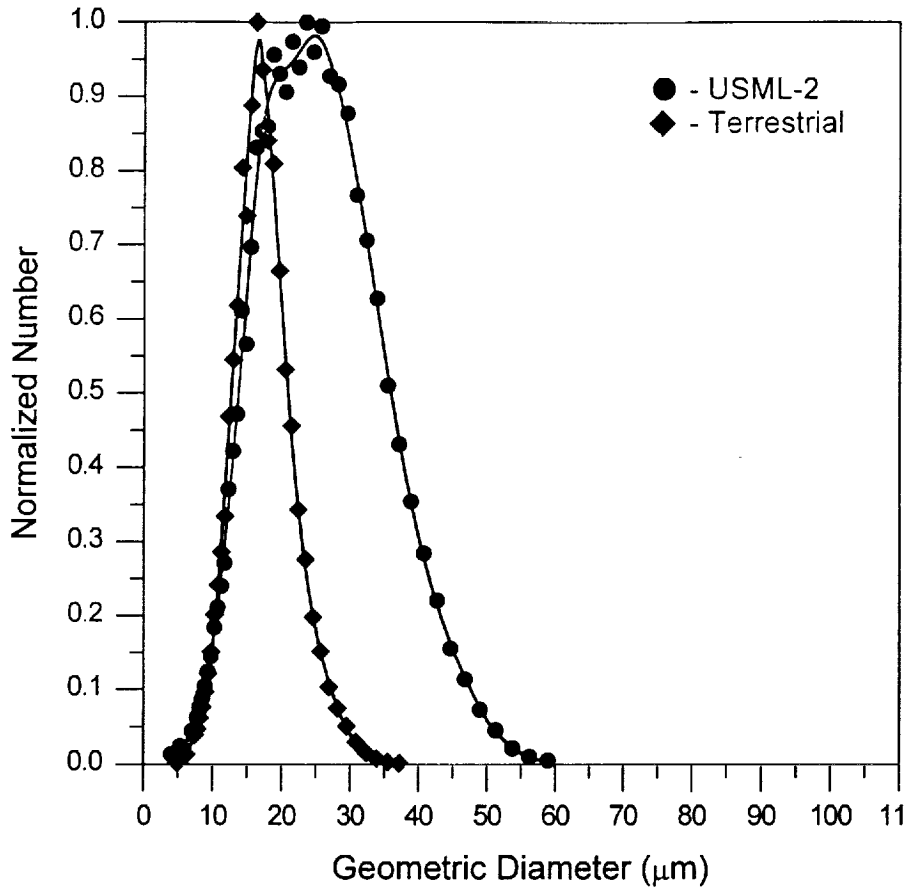

Figure 20. PSD's of Silicalite Illustrated in Figure 19

The catalytic activity of the external surface of the flight and the terrestrial control Silicalite crystals formed using untreated silica gel was measured. The test reaction was a carbon/carbon double bond isomerization of 2,4,4-trimethyl-1-pentene (2,4,4-TMP-1) to 2,4,4-trimethyl-2-pentene (2,4,4-TMP-2) at 175 °C. This reaction is catalyzed by weakly acidic silanol Si-OH groups (10). Molecules such as 2,4,4-TMP-1 do not, or hardly, enter the MFI (Silicalite) structure. This is an assumption based on the fact that the experimental diffusion coefficient of comparable molecules such as dibranched 2,2-dimethylbutane molecule at 175 °C is small (approximately $2*10^{-11}$ cm^2/s) (11,12). Conversion of 2,4,4-TMP-1 to 2,4,4-TMP-2 catalyzed by Si-OH groups on the external surface of Silicalite can, therefore, serve as a convenient method of determining the concentration of surface hydroxyl groups on Silicalite. This can be related to Silicalite crystal surface roughness, since as the roughness of the external surface increases, so does the concentration of surface hydroxyl groups (13). Silicalite was used in the catalytic test in the as-synthesized, uncalcined form in order to take additional advantage of TPA^+ template filling the channels in MFI structure (14). Figure 22 illustrates the results of the conversion of 2,4,4-TMP-1 on the external surface of Silicalite crystals. As shown in Figure 22, after 3 h of reaction, the flight crystals resulted in approximately 50% lower

conversion of 2,4,4-TMP-1 than their terrestrial controls with identical cumulative surface area. These results indicate a lower catalytic activity of the external surface of flight crystals in comparison to terrestrial control crystals. This implies a lower concentration of surface hydroxyl groups on the external surface of flight Silicalite, suggesting that flight crystals are "smoother" (less defects) that their terrestrial controls. This is consistent with the AFM results for zeolites A and X which show flight crystals to be geometrically "smoother".

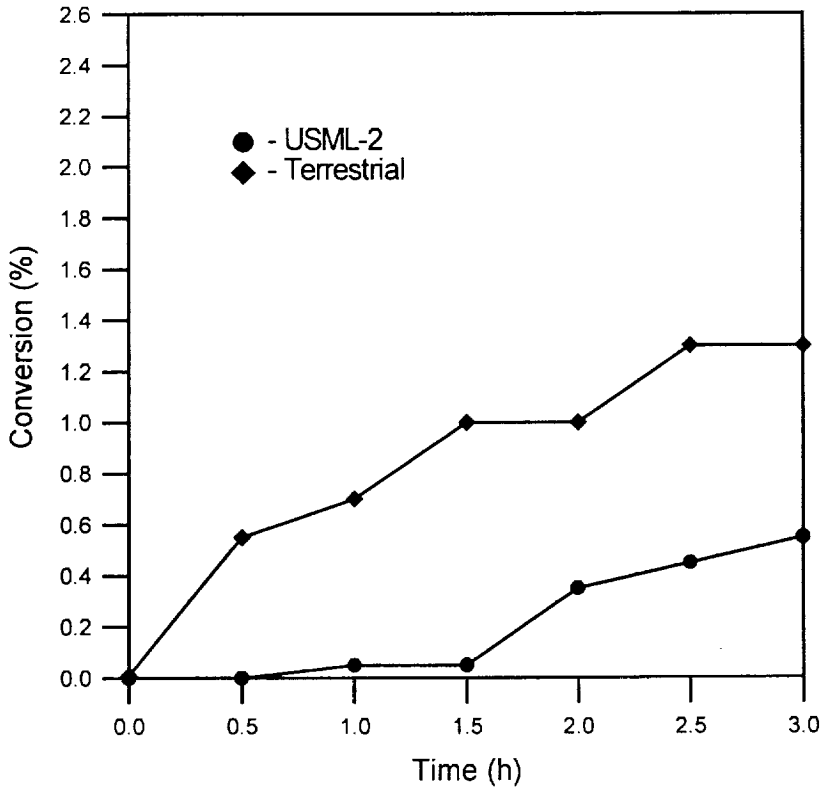

Figure 22. Catalytic Test Reaction (conversion of 2,4,4-trimethyl-1-pentene to 2,4,4-trimethyl-2-pentene on external surface of Silicalite at 175 °C) to Determine Terminal Silanol Groups on MFI

Heat treatment of silica gel granules in air at sufficiently high temperatures prior to synthesis, decreases the effective surface area of the silica source available for dissolution. This has proven to be an effective method of reducing nucleation of Mordenite crystals (15). In a similar manner nucleation control of Silicalite was attempted by heat treating silica gel at 700 °C for 20 hours prior to use in syntheses. Specific surface area of heat treated silica gel decreased from 750 to 320 m^2/g. Figure 23 shows the SEM micrographs of Silicalite crystals grown from heat treated silica in microgravity and 1g environments. PSD's for the products corresponding to Figure 23 are given in Figure 24.

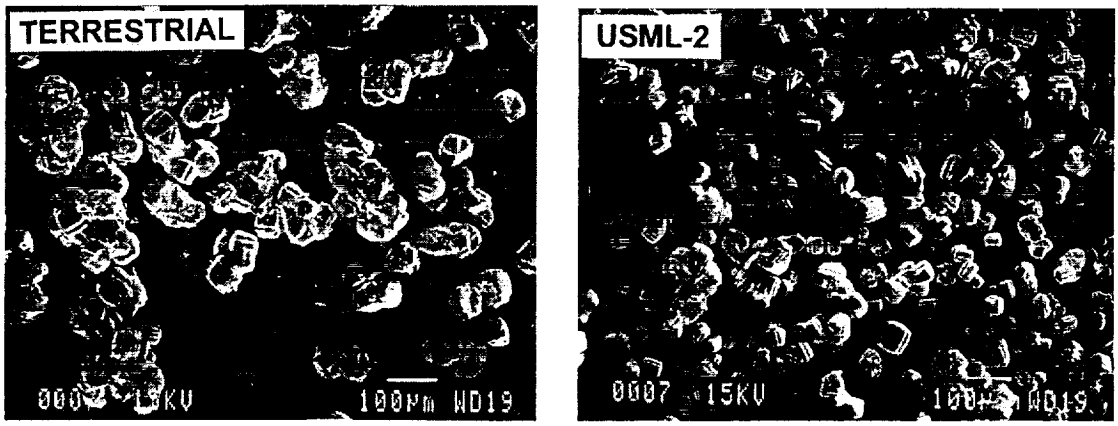

Figure 23. SEM Micrographs of Silicalite Crystallized from Heat Treated Silica Gel

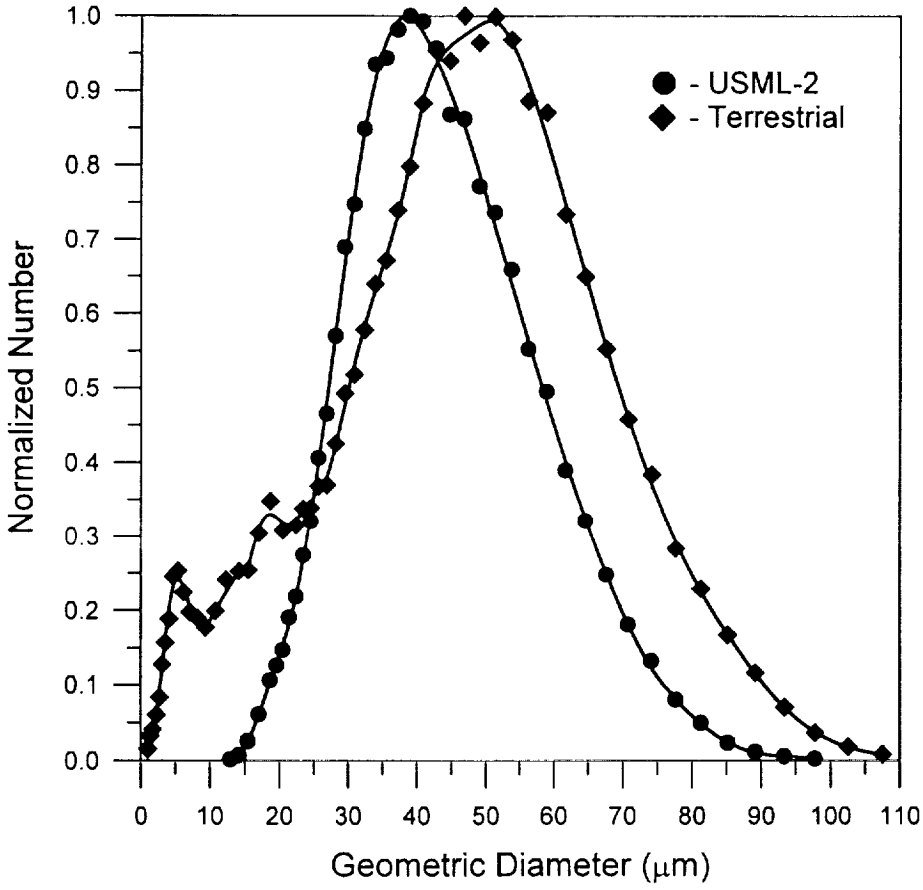

Figure 24. PSD's of the the Silicalite Illustrated in Figure 23

Comparison of the SEM micrographs shown in Figures 20 and 23 indicate a change of morphology of the terrestrial crystals from spherulitic agglomerates obtained using untreated silica gel to intergrown disks obtained using heat treated silica gel. This change of morphology combined with distinct size shift of PSD's to larger geometric diameters indicate a reduction of the nucleation of Silicalite crystals by using heat treated silica source. Similar morphologies and the size of the flight crystals grown using untreated silica gel (no nucleation control) and the terrestrial/control crystals grown using heat treated silica gel (reduction of nucleation rate), shown in Figures 20, 21, 23, and 24 indicate that microgravity environment resulted in a reduction of the nucleation rate. The flight crystals grown from heat treated silica gel show the same intergrown disks morphology as their terrestrial counterparts (nucleation rate is reduced in both cases). However, the flight crystals appear to be predominantly individual crystals or assemblies of a few crystals while the terrestrial crystals are predominantly in groups of larger agglomerates. The effects of these terrestrial/control agglomerates are seen in the PSD's shown in Figure 24. The observation of larger PSD'S for the terrestrial case is due to agglomeration. The product grown in microgravity is free of large agglomerates, resulting in a smaller PSD. However, when comparing the flight/heat treated silica gel and the flight/untreated silica gel samples, the heat treated samples are 52% larger.

The effect of agglomeration and sedimentation in the terrestrial samples was examined by cutting the Teflon liners (along the longitudinal axis) used in the synthesis of Silicalite in microgravity and 1g environments. Figure 25 shows the typical appearance of internal walls of the Teflon liners used to grow the terrestrial and the flight crystals. The effect of sedimentation in the terrestrial samples is obvious. Part of the product in the terrestrial autoclaves forms a scale, or cake attached to the internal wall of the Teflon liner. This region is circled to show the terrestrial agglomerates in Figure 25. However, the autoclave for the Silicalite samples grown in microgravity have a clean and smooth surface with no crystals, scale, or agglomerates attached. This shows the clear advantage of crystal growth in microgravity where absence of settling results in containerless-like processing.

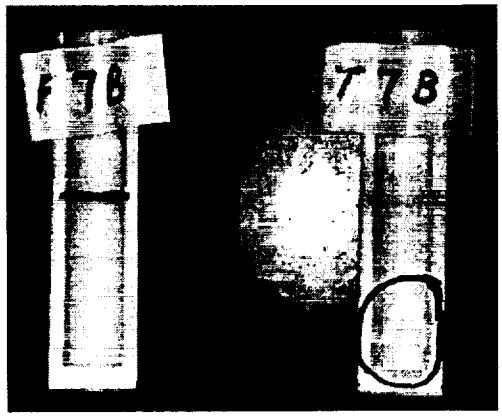

Figure 25. Teflon Liners of Flight (F7B) and Terrestrial (T7B) Autoclaves for Silicalite Synthesis from Heat Treated Silica Gel

3.4 Zeolite Beta

XRD patterns of the products from the zeolite Beta syntheses using untreated silica gel (no nucleation control) are typical for zeolite Beta (16) and show that the material is an intergrowth of two or three polymorphs. The SEM micrographs and PSD's of these products shown in Figures 26 and 27 do not show significant differences in either morphology or size between the terrestrial and flight samples of zeolite Beta. Both products crystallized in the form of polycrystalline round or slightly elongated aggregates 0.25-1.5 μm in geometric diameter.

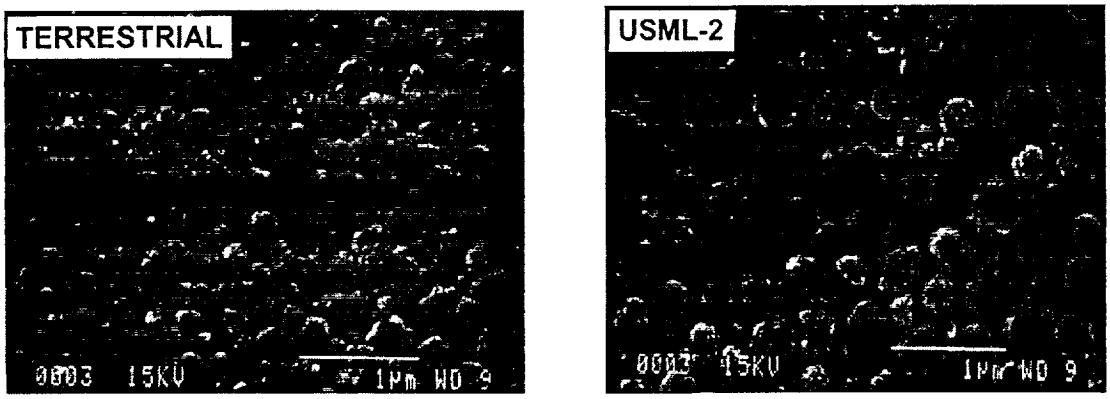

Figure 26. SEM Micrographs of Zeolite Beta from Silica Gel

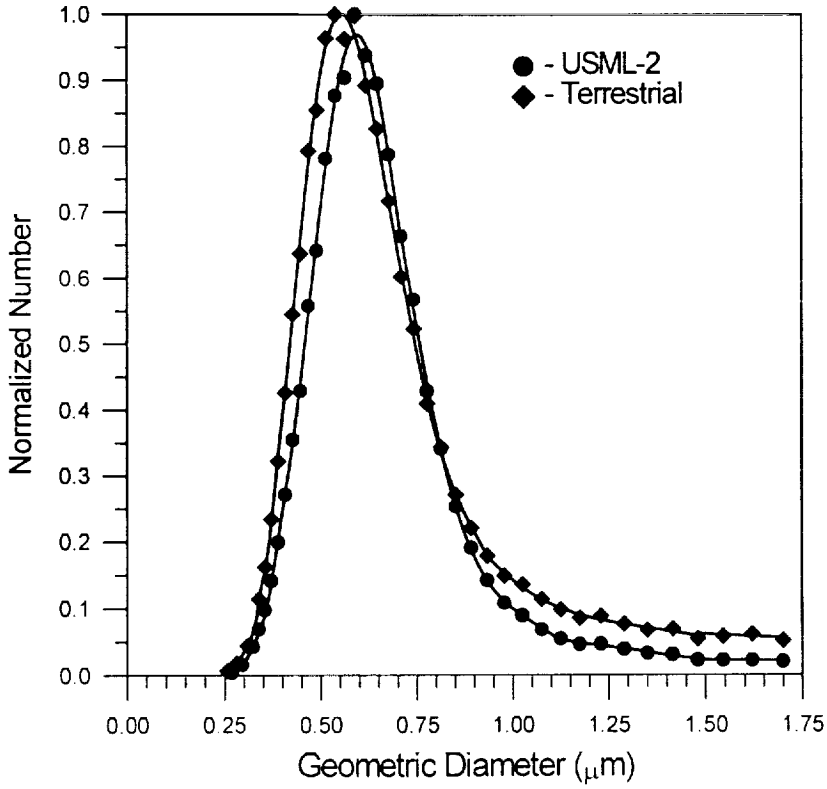

Figure 27. PSD's of Zeolite Beta Illustrated in Figure 26

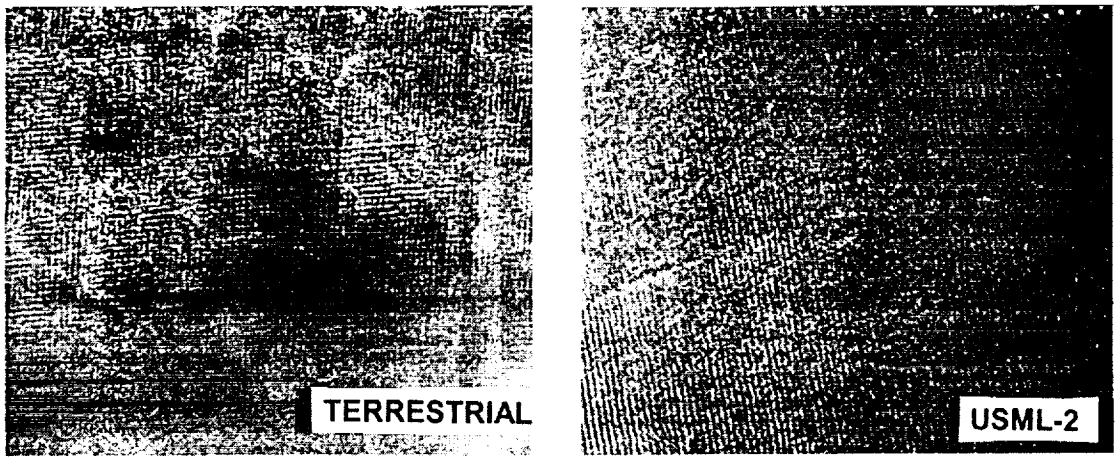

Figure 28. TEM Micrographs of Zeolite Beta from Silica Gel

Although the SEM micrographs and the particle size distributions look similar, Transmission Electron Microscope (TEM) micrographs of the same samples shown in Figure 28 clearly indicate that the zeolite Beta crystal grown in microgravity is structurally more perfect while the terrestrial sample has considerable line defects.

FTIR spectra of the same samples are shown in Figure 29. Intensity of a band at 3750 cm^{-1} for the flight sample is lower than for the terrestrial counterpart. This band is due to terminal hydroxyl group from the surface or at a defect site, and, therefore, the more intense band at 3750 cm^{-1} for the terrestrial sample may indicate more defect sites in the terrestrial sample, consistent with the TEM results.

The catalytic activity of the external surface of the flight and the terrestrial control zeolite Beta crystals formed using untreated silica gel was measured using the Brønsted acid catalyzed Claisen rearrangement of allyl 3,5-di-*tert*-butylphenyl ether followed by the cyclization of the primary product (2-allyl-3,5-di-*tert*-butylphenol) to 4,6-di-*tert*-butyl-2-methyldihydrobenzofuran in refluxing benzene (17).

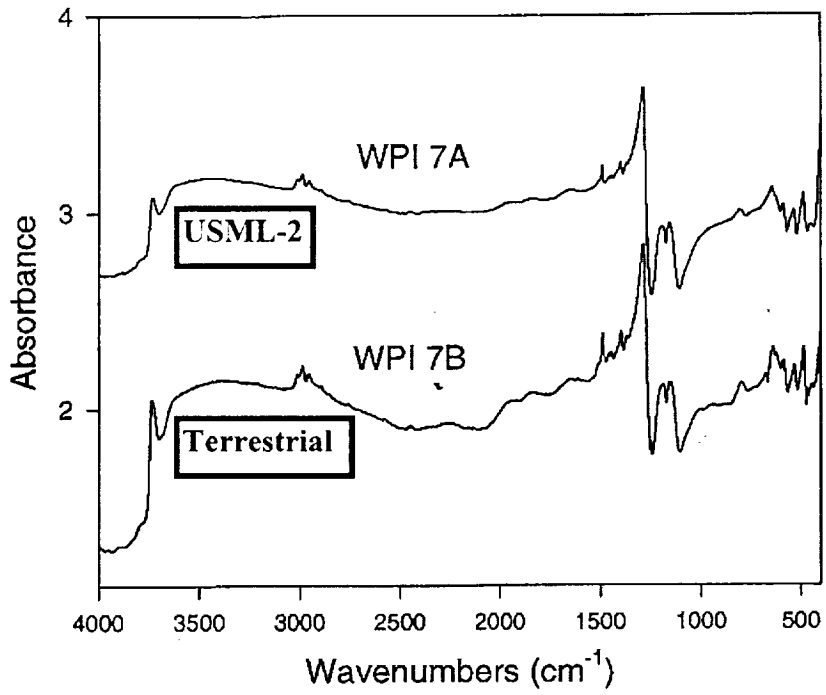

Figure 29. FTIR Analysis of Zeolite Beta from Untreated Silica Gel

The allyl 3,5-di-*tert*-butylphenyl ether probe molecule is of such dimensions (11.0x10.8x5.8 Å) that it cannot penetrate the straight channels (7.6x6.4 Å) of zeolite Beta (17). Before the test reaction was performed, as-synthesized flight and terrestrial/ control zeolite Beta crystals were simultaneously converted into an acid form by calcination to remove the TEA^+ template, followed by ion exchange with an ammonium salt to replace the Na^+ and activation to decompose NH_4^+. The Claisen rearrangement/ring closure reaction was then performed at 80 °C in refluxing benzene. Figure 30 illustrates the results. As shown in Figure 30 the selectivities to 4,6-di-*tert*-butyl-2-methyldihydrobenzofuran are high and identical (about 93%) for the flight and the terrestrial/control crystals. Also, conversion rates of allyl 3,5-di-*tert*-butylphenyl ether in both cases are practically identical, and within experimental error. These results indicate practically identical catalytic activity of external surface of the flight and the terrestrial/control zeolite H-Beta. This implies identical outer surface Brønsted acidity in the flight and the terrestrial/control crystals.

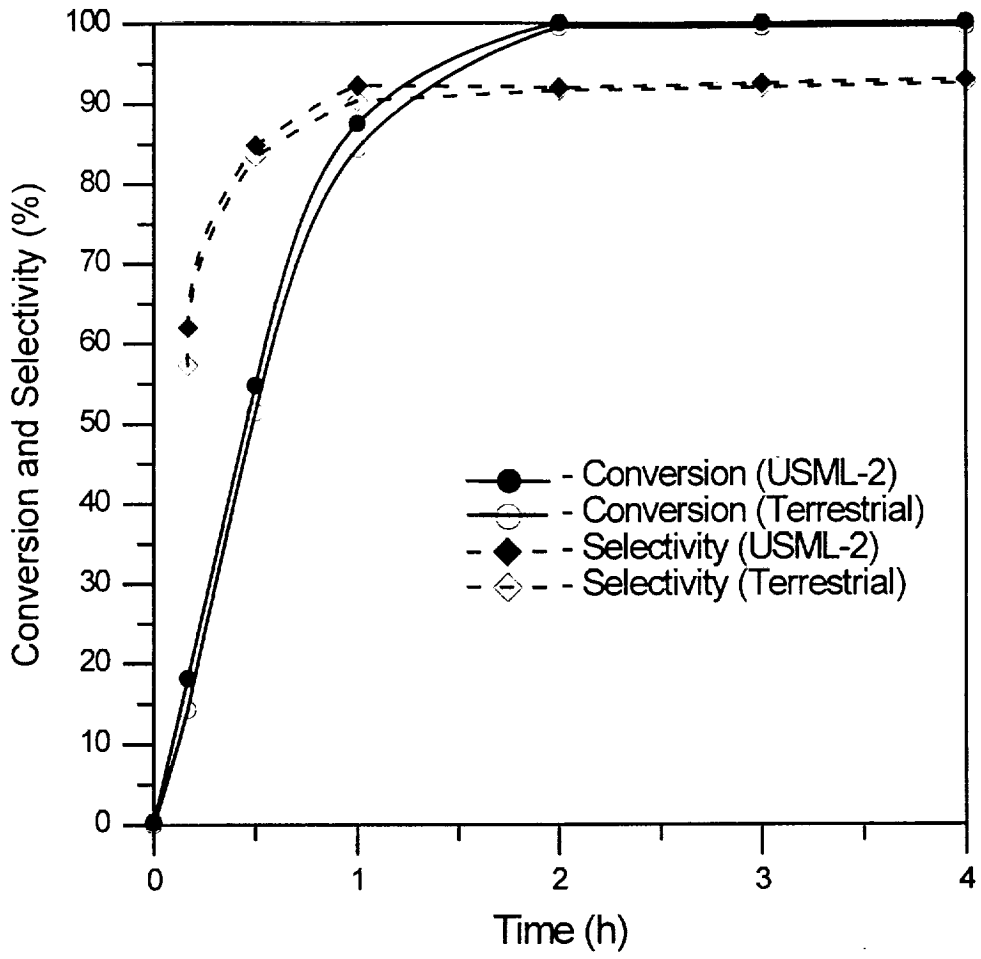

Figure 30. Catalytic Test Reaction (conversion of allyl 3,5-di-*tert*-butylphenyl ether and selectivity to 4,6-di-*tert*-butyl-2-methyldihydrobenzofuran obtained using zeolite H-Beta in refluxing benzene) to Determine the Outer Surface Brønsted Acidity

Activity of the micropore system of the flight and the terrestrial/control zeolite Beta crystals formed using untreated silica gel was tested in Meerwein-Ponndorf-Verley (MPV) reduction of 4-*tert*-butylcyclohexanone with 2-propanol (refluxing at 82.5 °C) to *cis*-4-*tert*-butylcyclohexanol. This reaction is believed to be catalyzed by Lewis acid sites related only to aluminum atoms located in the micropores and partially bonded to the framework (17). The 4-*tert*-butylcyclohexanone probe molecule is of such dimensions (6.4x5.8x9.6Å) that it can enter the pores of zeolite Beta (17). Before the test reaction, zeolite H-Beta crystals prepared from as-synthesized flight and terrestrial (control) samples were simultaneously activated to remove any organic matter deposited during the Claisen test reaction (Figure 30) for the activity of external surface. Figure 31 illustrates the results. As shown in Figure 31, the selectivities are high (about 93-95 %) and nearly identical for both flight and terrestrial/control samples within the experimental error of a few percent. The conversion rate and the percent conversion of 4-*tert*-butylcyclohexanone after 4 h of reaction are, however, much lower in the reaction

catalyzed by the flight crystals than by their terrestrial controls. These results indicate that the flight crystals have a lower catalytic activity in the MPV reduction reaction catalyzed by Lewis acid sites related only to "satellite" aluminum atoms partially bonded to the framework lattice. The results shown in Figure 31 indicate that the flight crystals appear to have significantly less Lewis acid sites than the terrestrial/control crystals as a result of identical ion exchange and thermal treatment history, or that the distribution of Lewis acid sites with different acid strengths is different in the flight crystals than in the terrestrial/controls. The presence of a lower number of Lewis acid sites ("satellite" aluminum atoms) in the flight crystals in comparison to the terrestrial/control crystals indicates fewer defects in the as-synthesized flight sample and/or much easier hydrolysis of aluminum (Al-O bond) from the framework of the terrestrial/control sample. Both explanations involve the notion of a more perfect lattice present in the flight crystals, consistent with the results of the TEM (Figure 28) and the FTIR (Figure 29) analysis.

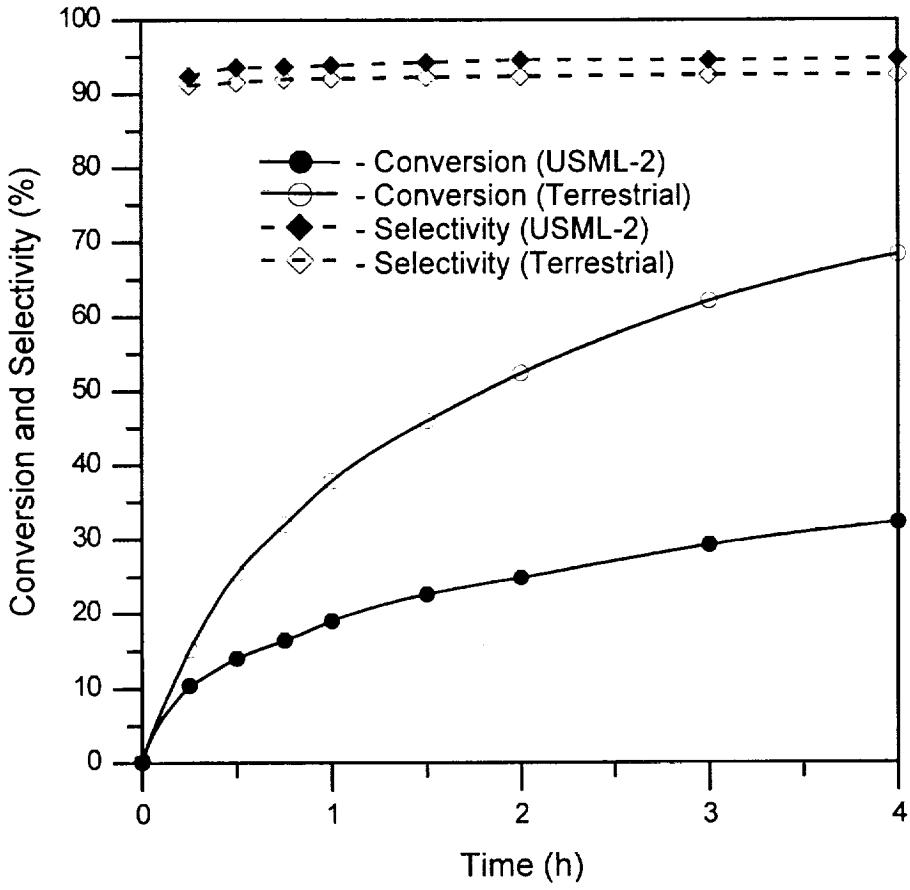

Figure 31. Catalytic Test Reaction (conversion of 4-*tert*-butylcyclohexanone to cis-4-*tert*-butylcyclohexanol using zeolite H-Beta in refluxing 2-propanol) to Determine Microporous Lewis Acidity

The Si/Al ratios of the zeolite Beta samples determined by SEM/EDX, (a semi-quantitative technique with an accuracy ~20%), indicate higher Al content in the flight sample than in the terrestrial/control counterpart, as shown in Table 3. The yield of zeolite Beta crystals is also higher in the flight than in the terrestrial/control sample, as seen in Table 3.

Table 3. Comparison of Si/Al Ratios and Yield of Flight (F) and Terrestrial/Control (T) Zeolite Beta crystals

Sample	Si/Al	Yield (g)
F (untreated silica source)	5.8	0.759
T (untreated silica source)	7.6	0.670
F (silica source heat treated at 850 °C)	7.1	0.820
T (silica source heat treated at 850 °C)	7.8	0.650

The morphology, the PSD's, and the purity of zeolite Beta synthesized using silica gel heat treated at 850 °C prior to syntheses are the same for crystals grown in microgravity or a 1g environment. However, flight crystals formed in higher yield and with higher Al content, as shown in Table 3. These results cannot be attributed to the formation of impurity phases because the XRD patterns for both products are the same.

The flight zeolite Beta product synthesized using a colloidal silica source (Ludox) was in loose powder form, similar to all the flight and the terrestrial/control zeolite Beta products grown from silica gel in both the untreated and the heat treated forms. The terrestrial zeolite Beta product grown using colloidal silica (Ludox), however, showed two distinct forms: a loose powder (herein referred to as "powder") and agglomerated solid chunks (referred to as "chunk"). These two different terrestrial forms were analyzed separately. X-ray data indicate that the flight zeolite Beta sample contained a very small amount of Chabazite and Faujasite impurity while the powder portion of the terrestrial/control sample contained a large amount of Faujasite impurity in addition to very small amounts of Chabazite impurity. The XRD did not reveal Faujasite in the chunk portion of the terrestrial/control sample. The PSD's of flight and two terrestrial portions of zeolite Beta samples were very similar to the PSD's of samples grown using silica gel. The reason for the presence of Faujasite in the flight sample and in loose portion of the terrestrial/control sample is unclear at this time, but may be due to local nonhomogeneous mixing pockets in the autoclaves.

3.5 Zeolite Glovebox Experiment (GBX-ZCG)

Zeolite Glovebox experiment was used to establish mixing procedures for the zeolite solutions to be processed in the ZCG facility. The results from the Glovebox experiment using clear autoclaves illustrated that real-time observation of the mixing process is necessary to ensure gel uniformity without excessive shear. Bubble formation,

inherent in the mixing process, was minimized with real-time observations including spinning the autoclaves if necessary.

In addition to establishing mixing protocols for the ZCG experiment, four GBX autoclaves contained reaction mixtures developed to produce zeolite A at low temperature. These were mounted on the outside surface of the ZCG furnace for crystal growth at 40 °C. No nucleation control agent was used in this synthesis in order to achieve 100% crystallinity of product at the end of synthesis. Visual observation of the progress of crystallization occurring in microgravity was therefore achieved for the first time. Visual observations verified the hypothesis that during synthesis gel will not settle and crystals will remain suspended in the reaction mixture. Figures 32 and 33 show the comparison of the flight and the terrestrial/control results from the zeolite A synthesis carried out at 40°C. As shown in Figure 32 the results from an on-orbit experiment do not differ significantly from the terrestrial duplicate, although PSD's of the flight samples appear to be shifted slightly towards larger sizes, (Figure 33). Similar results were observed for zeolite A synthesis with no nucleation control during USML-1.

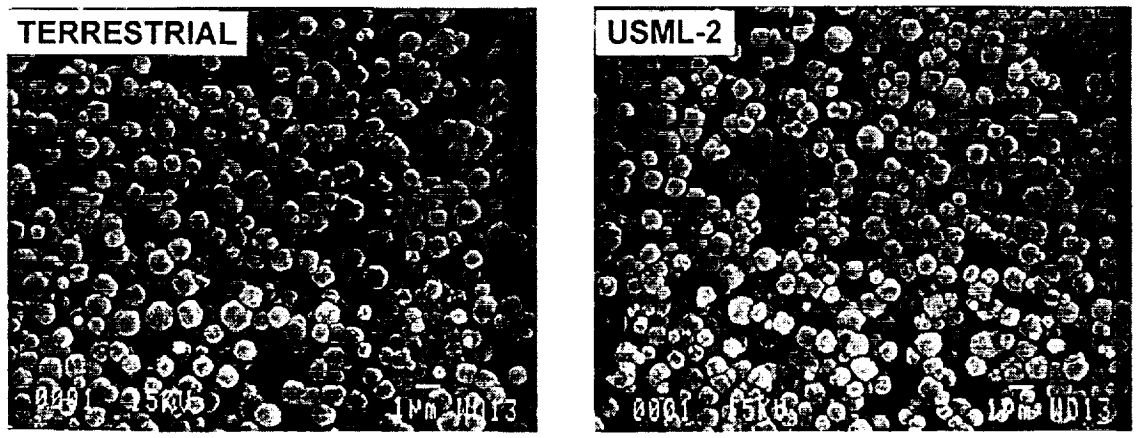

Figure 32. SEM Micrographs of Zeolite A Grown in Clear Glovebox Autoclaves

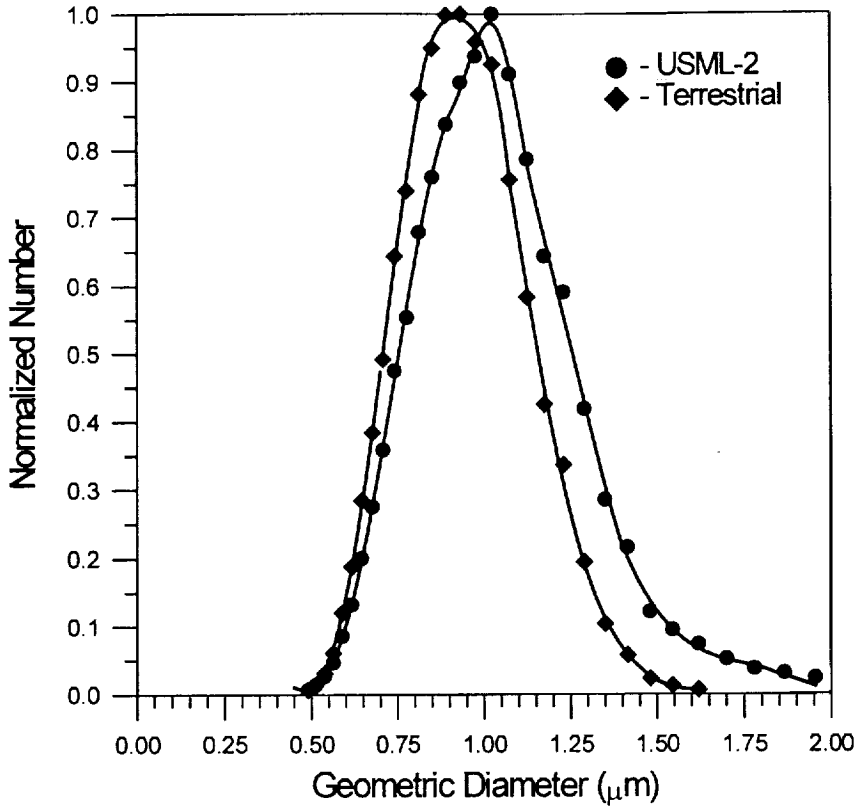

Figure 33. PSD's of Zeolite A Illustrated in Figure 32

4.0 CONCLUSIONS

Zeolite A samples grown in microgravity show enhanced size of largest crystals in comparison to their terrestrial/control counterparts. In addition, some amorphous material is present in many flight zeolite A samples grown in the presence of BIS. This indicates that fewer crystals nucleated in the flight samples and crystallization (conversion of amorphous gel into crystalline product) process took longer to complete in microgravity. Smaller unit cell volumes of the flight samples in comparison to the terrestrial/control samples appear to suggest fewer lattice defects in their structure.

Zeolite X samples are substantially larger in size in comparison to the terrestrial/control counterparts. This indicates that fewer crystals nucleated in flight samples. The size increase varies between 30-70%, depending on the type of formulation. Zeolite X crystals with size up to 215 μm (side of the octahedron) were obtained. The flight crystals have higher Si/Al ratios than their terrestrial counterparts and are more uniform.

Silicalite crystals grown from silica gel heat treated at 700 °C yielded larger crystals with an intergrown disks morphology. This morphology is different in

comparison to crystals synthesized from untreated silica gel, which grew as spherulitic agglomerates. This is due to reduced nucleation of Silicalite caused by slower dissolution rate of the heat treated silica gel in comparison with the untreated silica gel caused by its decreased specific surface area. Almost no agglomeration is observed in the flight samples due to lack (or reduction) of settling of the silica gel substrate and/or the Silicalite product.

Catalytic test of the Silicalite catalyzed 2,4,4-trimethyl-1-pentene isomerization to 2,4,4-trimethyl-2-pentene showed that the flight crystals exhibit lower catalytic activity of the external surface than the terrestrial/control crystals with the same cumulative external surface area. This indicates that the flight Silicalite crystals are "smoother" (have a lower surface roughness) than their terrestrial controls. This is consistent with the smoothness observed on AFM micrographs of zeolite A and X (Figures 7 and 18).

The TEM analysis of zeolite Beta show that the flight samples have fewer structural defects in comparison to the terrestrial/control samples. The silica source used in syntheses affected the quality, purity, and morphology of the final product. Yield and Al content in zeolite Beta obtained using untreated and heat treated silica gel were higher for the flight samples than the terrestrial controls. A different silica source (Ludox) resulted in large amounts of Faujasite impurity present in the flight zeolite Beta samples while the terrestrial/control samples had substantially lower Faujasite content. These results again illustrate the differences between the nucleation and the growth processes occurring in microgravity and 1g environments.

Zeolite H-Beta catalyzed Claisen rearrangement of allyl 3,5-di-*tert*-butylphenyl ether followed by cyclization of the intermediate 2-allyl-3,5-di-*tert*-butylphenol to 4,6-di-*tert*-butyl-2-methyldihydrobenzofuran showed identical catalytic activity of the external surface of flight and terrestrial/control crystals. This indicates nearly identical outer surface Brønsted acidity of the flight zeolite H-Beta crystals and their terrestrial controls.

Zeolite H-Beta catalyzed MPV reduction of 4-*tert*-butylcyclohexanone in the presence of 2-propanol showed that the flight crystals exhibit lower catalytic activity related to Lewis acid sites located in the micropores. These are due to aluminum atoms only partially bonded to the framework, suggesting that the flight crystals appear to have less structural defects than their terrestrial controls.

5.0 ACKNOWLEDGMENT

The authors acknowledge NASA for funding. Thanks are extended to the crew of STS-73, especially Kathryn Thornton and Catherine Coleman for a great job in orbit. In addition thanks are extended to Lisa McCauley of Battelle for her support, and Jack Ferraro (WPI), and the ZCG assembly crew at KSC: Ipek Guray, Teran L. Sacco, Michelle Marceau, and Robert Whitmore (Battelle).

6.0 REFERENCES

1. Chemical Week, 35, June 5, 1996
2. Pennisi, E., *Science News*, **140**, 22 (1992)
3. Schmidt, W., CASIMIR-1 Mission, Final Report, Intospace (1992)
4. Sano, T., Mizukami, F., Kawamura, M., Takaya, H., Mouri, T., Inaoka, W., Toida, Y., Watanabe, M. and Toyoda, K., *Zeolites*, **12**, 801 (1992)
5. Sacco, A. Jr., Thompson, R.W. and Dixon, A.G., Int. SAMPE Conference, **18**, 330 (1986)
6. Sand, L.B., Sacco, A. Jr., Thompson, R.W. and Dixon, A.G., *Zeolites*, **7**, 387 (1987)
7. Sacco, A., Jr., Baç, N., Warzywoda, J., Guray, I., Thompson, R.W. and McCauley, L.A., Space Technology and Applications International Forum, AIP Conference Proceedings 361, Albuquerque, NM, January 7-11, 1996
8. Sacco, A., Jr., Baç, N., Coker, E.N., Dixon, A.G., Warzywoda, J. and Thompson, R.W., Joint L+1 Year Science Review of USML-1 and USMP-1, NASA Conference Publication 3272, May 1994
9. Breck, D.W., *Zeolite Molecular Sieves*, J.Wiley, New York (1974)
10. van der Puil, N., *Development and Catalytic Testing of Zeolitic Coatings*, Ph.D. Thesis, TU Delft (1997)
11. Cavalcante, C.L. and Ruthven, D.M., *Ind. Eng. Chem.Res.*, **34**, 185 (1995)
12. Weitkamp, J., Kromminga, T. and Ernst, S., *Chem.-Ing.-Tech.*, **64**, 1112 (1992)
13. Coker, E.N., Koegler, J.H. and Jansen, K.C., 19th BZA Annual Meeting, Edinburgh, July 21-26, 1996
14. Lok, B.M., Cannan, T.R. and Messina, C.A., *Zeolites*, **3**, 282 (1983)
15. Warzywoda, J., A.G. Dixon, R.W. Thompson, and A. Sacco Jr., *J. Mater. Chem.*, **5**, 985 (1995)
16. Newsam, J.M. , M.M. Tseang, N.T. Koetsier, and C.B. de Gruyter, *Proc. R. Soc. Lond. A*, **420**, 375 (1988)
17. Creyghton, E., *New Applications of Zeolite Beta in Selective Catalytic Hydrogenations*, Ph.D. Thesis, TU Delft (1996)